PHYSICAL REVIEW D **93,** 113017 (2016)

Lepton number violation and 'Diracness' of massive neutrinos composed of Majorana states

Janusz Gluza,[1] Tomasz Jeliński,[1] and Robert Szafron[2]

[1]*Institute of Physics, University of Silesia, Uniwersytecka 4, 40-007 Katowice, Poland*
[2]*Department of Physics, University of Alberta, Edmonton, Alberta, Canada T6G 2G7*

(Received 18 February 2016; published 29 June 2016)

Majorana neutrinos naturally lead to a lepton number violation (LNV). A superposition of Majorana states can mimic Dirac-type neutrinos, leading to lepton number conservation. Using the example of specific observables related to high- and low-energy processes, we demonstrate how the strength of LNV correlates with neutrino parameters, such as *CP* phases, flavor mixings, and mass ratios. We stress the coaction of low- and high-energy studies for quantitatively testing phenomenological models. Second, we conclude that in order to fully study the role of heavy neutrinos in the search for new physics signals, a departure from trivial scenarios assuming degeneracy in mass and no flavor mixing or *CP* phases becomes necessary for a proper physical analysis.

DOI: 10.1103/PhysRevD.93.113017

I. INTRODUCTION

The neutrino oscillation phenomenon established that at least two out of the three known neutrinos are massive, though their masses are very tiny, at most at the electronvolt level, $m_\nu \sim \mathcal{O}(1)$ eV. It was a tremendous effort that led to this result as experimental studies of neutrino physics face the challenge of low event statistics for an already scarce set of observables. It started around half a century ago with the pioneering Homestake experiment and the so-called solar neutrino problem [1], and ended with last year's Nobel award for Takaaki Kajita and Arthur B. McDonald (Super-Kamiokande and SNO collaborations [2,3]), "for the discovery of neutrino oscillations, which shows that neutrinos have mass".

Evidence of new phenomena involving neutrinos often stirs up a lot of attention in both the physics community and the public media, although sometimes for no good reason; cf. the 17-keV neutrino (dubbed a Simpson's neutrino) signal in tritium decays [4,5], the OPERA faster-than-light neutrino controversy [6,7], or positive neutrinoless double beta-decay signals [8] (see also comments in Ref. [9]). Certainly, we can expect more such situations in the future, as neutrino experiments explore by definition *weak* effects and belong to the most challenging endeavors in physics.

Though the Large Hadron Collider (LHC) collides protons and deals predominantly with hadron effects, it is also sensitive to electroweak and new physics (NP) effects. One of the exciting NP options is the TeV heavy neutrino physics, $M_N \sim \mathcal{O}(1)$ TeV. Heavier particles can hardly be produced at a detectable level in collisions or observed indirectly in precise low-energy experiments.

In theory, heavy neutrino states are commonly embedded within the seesaw mass mechanism [10–13]. It explains the smallness of the known neutrino masses using the notion of Majorana states where lepton number violation (LNV) is present. A typical example is the neutrinoless double beta decay $(\beta\beta)_{0\nu}$ considered in this work, where a nuclear transition ends with two electrons in the final state [14–16]. Alternatively, in the inverse seesaw mechanism (depending on the choice of mass parameters) either Majorana or Dirac neutrinos can appear [17,18]. The question of whether neutrino states are of Majorana or Dirac type (or maybe a mixture) is a core problem in particle and astroparticle physics [19–21]. Theories involving Dirac-type particles obey lepton number conservation (LNC); in the inverse seesaw scenario, lepton number violation can vary naturally and may be substantial or negligible. Apart from the LNV issue, massive neutrinos (regardless of their type) can lead to the appearance of charged lepton flavor violation (CLFV) [22]. Here a change of the charged lepton flavor requires nontrivial neutrino mixing matrices.

As even a single unambiguous LNV or CLFV event detection would be a signal of NP, there are many efforts to upgrade or create new experimental setups. Present bounds for low-energy CLFV signals, such as nuclear μ to e conversion, will become more stringent at the so-called intensity frontier experiments [23,24]. The same is true for $(\beta\beta)_{0\nu}$ experiments; see, e.g., Ref. [25].

We show that limits on the low-energy processes are essential for LHC searches and give deep insight into neutrino scenarios. In these studies an investigation of nontrivial parameters—such as nondiagonal neutrino mixings, nonzero *CP* phases, or nondegenerated neutrino masses—is crucial.

We consider a pending and relevant topic: how much can we simplify models in an experimental analysis, for instance, when searching for right-handed currents and heavy Majorana/Dirac neutrinos? This issue is important, especially in the context of such searches by the CMS and ATLAS collaborations.

In the next and main section we track the whole discussion and above-mentioned issues in the context of the $pp \to lljj$ process. This process (coined the "golden" or "smoking-gun" process) is a good probe for NP due to its sensitivity to right-handed currents. They are not suppressed if heavy neutrinos exist. We will consider such heavy *Majorana* neutrinos and observe how composed Majorana neutrinos mimic Dirac states, and how they affect LNV. As will be shown, $pp \to lljj$ connects three different high- and low-energy experiments and is a perfect workhorse for a general discussion of LNV effects and mutual constraints imposed on NP model parameters. We conclude in Sec. III with a summary and outlook. The paper includes four appendices. In Appendix A we discuss some further details relevant for the Majorana neutrino processes at high energies, focusing on $pp \to lljj$ and $e^-e^- \to W_2^-W_2^-$. In Appendix B, current and planned limits in searches for CLFV low-energy processes are given, with specific focus on $\tau \to e\gamma$ which must be considered in the context of the neutrino mixing parametrization considered in the main text. Appendix C includes the analytic parametrization of the effective two-heavy-Majorana-neutrino mixing and its connection with *CP* parities and phases of heavy neutrinos. In Appendix D a short summary of Weyl, Dirac, and Majorana types of neutrinos is given, with a focus on the theoretical concepts of neutrino mass matrices and their connection with the "Diracness" of neutrinos and the golden $pp \to lljj$ process.

II. DISCUSSION AND RESULTS

Our discussion is based on the following Lagrangian:

$$\mathcal{L} = \frac{g}{\sqrt{2}} \sum_{a=1}^{3} \overline{\nu}_a \gamma^\mu P_L (U_{\mathrm{PMNS}})^\dagger_{aj} l_j W^+_{1\mu} + \mathrm{H.c.} \qquad (1)$$

$$+ \frac{\tilde{g}}{\sqrt{2}} \sum_{a=1}^{3} \overline{N}_a \gamma^\mu P_R (K_R)_{aj} l_j W^+_{2\mu} + \mathrm{H.c.}, \qquad (2)$$

where N_a stands for massive *Majorana* states (most naturally, in popular models based on left-right gauge symmetry there are three M_a heavy neutrinos). The term (1) describes the standard model (SM) physics of charged currents. It includes the celebrated neutrino mixing matrix U_{PMNS}, responsible for neutrino oscillation phenomena. The term (2) is responsible for nonstandard effects connected with heavy neutrinos M_a, their mixing matrix K_R, and right-handed currents mediated by an additional charged gauge boson W_2. These are three types of modeled unknowns. For models and phenomenology of heavy neutrinos without right-handed currents, see, for instance, Refs. [26,27].

The main NP contribution to the $pp \to lljj$ process is sketched in Fig. 1. It is a prominent process that was discussed long before the LHC, at the dawn of the Tevatron era [28]. In this process, same-sign (SS) leptons indicate LNV, which can be naturally explained by Majorana-type neutrinos. If the excess is only seen with opposite-sign (OS) leptons, the situation is more complicated. According to Feynman rules [29,30], a virtual Majorana particle can change the lepton number on the way from one vertex to another, which may result in the production of the same charged dileptons. However, as we will see, since Majorana virtual states act in a coherent way, much depends on couplings and the neutrino mixing matrix elements K_R.

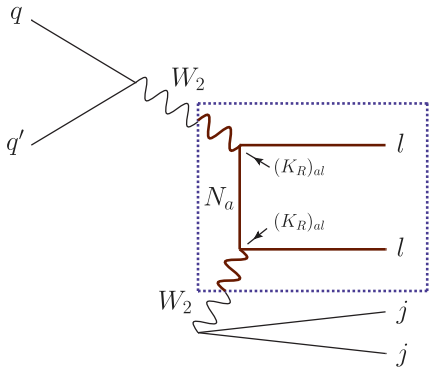

FIG. 1. Feynman diagram responsible for the "golden" $pp \to lljj$ signal. For Majorana neutrinos two signals are possible with same-sign leptons $pp \to W_2^\pm \to l_i^\pm N_a \to l_i^\pm l_j^\pm jj$ and opposite-sign leptons $pp \to W_2^\pm \to l_i^\pm N_a \to l_i^\pm l_j^\mp jj$. In the internal frame two related LNV processes can be identified: $ll \to W_2W_2$ (possible at the future lepton colliders) and $W_2^-W_2^- \to e^-e^-$ [a part of the low-energy neutrinoless nuclear double beta decay $(\beta\beta)_{0\nu}$].

In Fig. 1 two additional processes $e^-e^- \to W_2^-W_2^-$ and $W_2^-W_2^- \to e^-e^-$ can be spotted. The first process can be a good option for LNV searches at future electron colliders, while the second one is a weak-interaction part of the neutrinoless double beta-decay $(\beta\beta)_{0\nu}$ experiment. All three processes have the same couplings, though they differ in channels and characteristic kinematics. That is why $pp \to lljj$ depends strongly on experimental bounds derived from $(\beta\beta)_{0\nu}$.

Now we look at the details of the low-energy $(\beta\beta)_{0\nu}$ process; for other important low-energy processes, see Appendix B. In $(\beta\beta)_{0\nu}$, the light- and heavy-neutrino contribution to the half-life reads

$$\frac{1}{T^{0\nu}_{1/2}} = G|m^\nu + m^N|^2, \qquad (3)$$

where G includes all nuclear parameters. For light neutrinos, the effective mass term m^ν is proportional to the light neutrino masses m_i, namely, $m^\nu = \sum_{i=1}^{3} (U_{\mathrm{PMNS}})^2_{ei} m_i$. The heavy-neutrino exchange due to the interaction (2) yields a term inversely proportional to the heavy neutrino masses M_a ($|p^2| \sim 100$ MeV^2),

$$m^N = \left(\frac{\tilde{g}}{g}\right)^4 \left(\frac{M_{W_1}}{M_{W_2}}\right)^4 |p|^2 \sum_a \frac{(K_R)^2_{ea}}{M_a}. \quad (4)$$

Two sorts of cancellations are possible: either between light and heavy contributions, or inside each of them separately [31–42]. In m^ν and m^N the mixing matrices $U_{\rm PMNS}$ and K_R are squared, so without complex phases they always contribute positively. Cancellations appear if nonzero CP phases are involved. m^ν depends on the absolute value of the lightest neutrino mass and mass hierarchies related to the neutrino oscillation analysis [40,43,44]. Allowing for the whole range of CP phases in $U_{\rm PMNS}$, the results for m^ν can span from zero to the values of $T^{0\nu}_{1/2}$ allowed by $(\beta\beta)_{0\nu}$ experiments [35,40,45,46]. Interestingly, negligible m^ν contributions to $(\beta\beta)_{0\nu}$ are possible only in the case of the normal light-neutrino mass hierarchy [35,40,43,44]. In the inverted mass hierarchy m^ν cannot reach zero. In this case results and constraints on the NP parameters coming from m^N presented below would be relaxed due to possible CP effects in $U_{\rm PMNS}$ and $m^\nu - m^N$ cancellations.

To proceed further and calculate the $(\beta\beta)_{0\nu}$ half-life, the NP parameters K_R and M_i must be specified. In what follows we will consider two physically interesting scenarios and their variants.

(A) $(K_R)_{aj} = \delta_{aj}, M_a = M_{W_2}/2$, and $M_{W_2} = 2.2$ TeV. This is the simplest case of degenerate heavy neutrinos without flavor mixings. It was used in the CMS $M_a - M_{W_2}$ exclusion analysis in the context of the excess in $\sigma(pp \to eejj)$ at the invariant mass of about 2.2 TeV [47].

(B) Masses as in (A), $M_a = M_{W_2}/2$, and $M_{W_2} = 2.2$ TeV. K_R includes the simplest two-variable parametrization mixing matrix (one nontrivial rotational mixing angle θ_{13} and one CP phase ϕ_3),

$$K_R = \begin{pmatrix} \cos\theta_{13} & 0 & \sin\theta_{13} \\ 0 & 1 & 0 \\ -e^{i\phi_3}\sin\theta_{13} & 0 & e^{i\phi_3}\cos\theta_{13} \end{pmatrix}. \quad (5)$$

(C) As in (B), but with $M_{W_2} = 3$ TeV.

(D) As in (B), but with $\tilde{g}/g = 0.6$.

In case (A), there are no mixings. In case (B) they occur between N_1 and N_3, leading to possible electron-tau CLFV effects; see Eq. (2) and Appendix B. N_2 does not mix here and remains of Majorana type. Its LNV effects could then be detected in some process, e.g., $\mu^-\mu^- \to W_2^- W_2^-$, analogously to the $e^-e^- \to W_2^- W_2^-$ case considered in Appendix A. In our study K_R is always unitary and therefore it leaves no room for additional light-heavy neutrino mixings that are tightly constrained or need special constructions [48,49].

Figure 2 shows predictions for $(\beta\beta)_{0\nu}$ in scenarios (A)–(D) for $(\beta\beta)_{0\nu}$ when the m^N term dominates. In cases

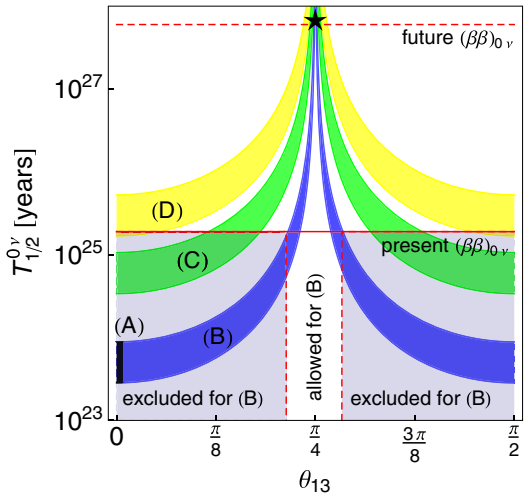

FIG. 2. "Christmas Tree" exclusion plot for m^N dominating the $(\beta\beta)_{0\nu}$ half-life $T^{0\nu}_{1/2}[^{76}\mathrm{Ge} \to {}^{76}\mathrm{Se}]$ as a function of θ_{13}. $\eta_{CP}(N_1) = -\eta_{CP}(N_3) = i$, $\phi_3 = \pi/2$, and $M_{1,2,3} = M_{W_2}/2 = 1.1$ TeV. The star represents the infinite half-life Dirac scenario (maximal θ_{13} mixing). The bands correspond to different evaluations of the nuclear matrix elements [36]. The excluded region (below the solid horizontal line) comes from Ref. [53]. The dashed horizontal line represents the expected future bound from the Majorana + GERDA experiment [25].

(A) and (B), we take a relatively small $M_{W_2} = 2.2$ TeV. This is a value of the $eejj$ invariant mass for which an excess in $\sigma(pp \to eejj)$ was reported by CMS during the LHC Run 1 [47]. However, it is in an excluded region for scenarios in which $g = \tilde{g}$ and heavy neutrinos do not mix and are degenerate in mass [47]. We compare this case with LNV low-energy predictions for the same scenario and for the scenario in which heavy neutrino mixings and nondegenerate masses are allowed. In Fig. 2, we consider cases (A)–(D) with degenerate neutrino masses and N_1, N_3 which have opposite CP parities, $\phi_3 = \pi/2$. (CP parities of neutrinos are strictly connected with the imaginary part of neutrino mixing elements; see Appendix C and Refs. [50–52].)

The results are interesting. First, let us note that the typical scenarios tested by CMS/ATLAS with no mixings and degenerate heavy neutrinos are in the excluded region (A) in Fig. 2. Second, the flavor mixing θ_{13} in case (B) is limited to the region close to $\pi/4$ for which LNC is restored. It can be seen directly using the parametrization shown in Eq. (5), for which Eq. (2) explicitly reads

$$\mathcal{L}_{\rm RHC} = \frac{\tilde{g}}{\sqrt{2}} \overline{N}_{\rm eff} \gamma^\mu P_R l_1 W^+_{2\mu} + \text{H.c.}, \quad (6)$$

where

$$N_{\rm eff} = (\cos\theta_{13} N_1 - e^{i\phi_3}\sin\theta_{13} N_3). \quad (7)$$

For $\theta_{13} = \pi/4, \phi_3 = \pi/2$ we have $N_{\rm eff} = (N_1 + iN_3)/\sqrt{2}$. This is a definition of the Dirac neutrino composed of two

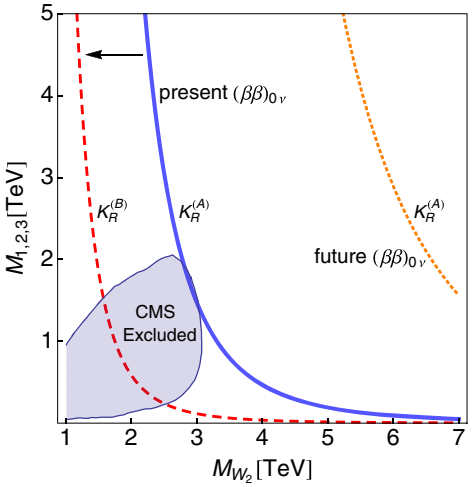

FIG. 3. The CMS vs m^N dominant $(\beta\beta)_{0\nu}$ exclusion limits on the masses of W_2 and N_a in the case when $(K_R)_{aj} = \delta_{aj}$ as in the (A) scenario. The shaded region is excluded by the CMS data related to $pp \to eejj$ at the LHC Run 1 [47]. Present $(\beta\beta)_{0\nu}$ experiments exclude the region under the blue solid curve. The dotted orange curve corresponds to a future bound on $T^{0\nu}_{1/2}$ [25]. For comparison, when the mixing matrix K_R is of the form (5) with $\theta_{13} = 0.9 \times \pi/4$ and $\phi_3 = \pi/2$, only the region under the dashed red curve is excluded. There are no available LHC data exclusion analyses for such "almost" Dirac neutrinos.

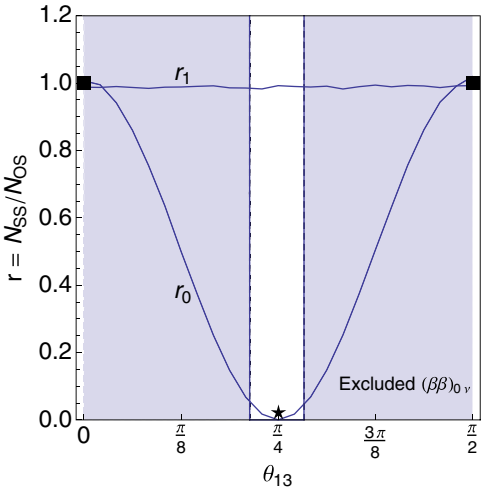

FIG. 4. Dependence of r_0 and r_1 on θ_{13} for case (B) for two neutrinos with opposite CP parities, $\eta(N_1) = -\eta(N_3) = i$ [$\phi_3 = \pi/2$ in Eq. (7)]. The subscript 0(1) of $r_{0(1)}$ means that there is a 0(1) GeV mass splitting between the N_1 and N_3 states. The star represents a scenario with $\theta_{13} = \pi/4$ equivalent to one Dirac heavy neutrino. Black squares correspond to pure Majorana states (no interferences). The shaded region is already excluded by the m^N dominant $(\beta\beta)_{0\nu}$ experimental data given in Fig. 2.

Majorana degenerated states with opposite CP parities; see Appendix C and Ref. [50]. In this case N_1 and N_3 Majorana neutrinos give opposite contributions to m^N of equal weight, $\sum_a (K_R)^2_{ea} = 1^2 + i^2 = 0$ (infinite half-life time). In our opinion this is the easiest way to see how two Majorana neutrinos act as the Dirac state and effectively lead to LNC. Third, we can see from Fig. 2 that scenario (D) with $g \neq \tilde{g}$ is not constrained by present $(\beta\beta)_{0\nu}$ data. This scenario is more suitable as far as grand-unified-theory unification of couplings is concerned [54,55].

Assuming again that right-handed currents and m^N dominate $(\beta\beta)_{0\nu}$, Fig. 3 shows how a strong low-energy process can influence heavy mass parameters, compared to the LHC Run 1 studies. The CMS exclusion area for the (A) scenario is well within the exclusion region given by the present $(\beta\beta)_{0\nu}$ data. For the case (B) when nondiagonal K_R elements are assumed, the limits on M_{W_2} and M_a coming from $(\beta\beta)_{0\nu}$ are much weaker. For example, when $\theta_{13} = 0.9 \times \pi/4$ and $\phi_3 = \pi/2$, which is a small distortion from the pure Dirac neutrino case (such states are also called pseudo-Dirac neutrinos), the masses of N_a and W_2 can be as low as 1 and 2 TeV, respectively; see Fig. 3.

We expect that allowing a wider range of mixing parameters in the CMS analysis of $pp \to eejj$ [47] would analogously relax their bounds on M_{W_2} and M_a. That is why it is desirable that the LHC collaborations include more complicated but natural and less tuned mixing scenarios in future heavy neutrino analysis.

Let us come back to the LNV discussion in the LHC physics and introduce a $r = N_{SS}/N_{OS}$ parameter that characterizes nonstandard contributions to $\sigma(pp \to eejj)$; see Refs. [55,56] for earlier studies of r dependences in another contexts. Here $N_{SS}(N_{OS})$ is the number of SS (OS) events, respectively. $r = 0$ corresponds to the LNC SM case. The results are shown in Fig. 4 for the case (B) which includes neutrino mixing and CP phase parameters. Neutrinos N_1, N_3 contribute with different weights in the vertices in Fig. 1; see Eqs. (6) and (7). If neutrinos are nondegenerate, additional weight factors appear. In this case, the lines in Fig. 4 would not be symmetric over $\theta_{13} \in (0, \pi/2)$. Both neutrinos interfere, leading to different values of r. For the Dirac case, denoted by the star on the bottom ($r = 0$), the mixing between two Majorana neutrino states should be maximal, $\theta_{13} = \pi/4$, so the CP phase $\phi_3 = \pi/2$. For the two top black squares, there is no mixing among neutrino states and the neutrino is purely of Majorana nature ($r = 1$, maximal LNV). If r is small [as dictated by $(\beta\beta)_{0\nu}$ bounds in Fig. 2], the lepton number is slightly broken and we get a pseudo-Dirac neutrino. The line r_1 in Fig. 4 shows that even a small nondegeneracy of neutrino Majorana states at the GeV level spoils the interference effects (neutrino decay widths are ~MeV). A similar effect occurs when two neutrinos have the same CP parities, $\eta(N_1) = \eta(N_3)$. Then the dependence on the mixing angle θ_{13} cancels out from physical observables like r. Let us also note that r does not change when $\tilde{g}$ deviates from g. It is a consequence of the fact that both N_{OS} and N_{SS} scale as $\tilde{g}^2$. Further technical details related to r and its dependence on the mixing matrix K_R, decay widths, and masses are discussed in Appendix A. Based on the results

TABLE I. "Diracness" of neutrino states composed of Majorana massive states measured by the $r = N_{SS}/N_{OS}$ parameter in $pp \to lljj$; see Fig. 4. $\Delta M_{ab} = M_a - M_b$ and $\Gamma_{a,b}$ are Majorana neutrino mass splittings and decay widths, respectively.

$\Delta M_{ab}/\max_{a,b}(\Gamma_a, \Gamma_b)$	r	ΔL violation	nature
0	0	0	Dirac
$\ll 1$	small	moderate	pseudo-Dirac
~ 1	large	substantial	Majorana
$\gg 1$	1	maximal	Majorana

shown in Fig. 4, different scenarios are summarized in Table I.

Here we considered the dependence of r on physical parameters, such as masses of heavy neutrinos, decay widths, and CP parities. In Ref. [55] it has been shown that in some models r can be related directly to the neutrino mass matrix entries. In the case of the inverse seesaw mechanism $r \simeq \mu_R^2/(\mu_R^2 + 4M_N^2)$. See Appendix D for various mass matrix parametrizations and Ref. [55] for further details.

III. SUMMARY AND OUTLOOK

Assuming right-handed currents, we have shown in a couple of related processes how the strength of LNV varies with the parameters of heavy Majorana neutrinos. In extreme cases, Majorana neutrinos effectively do not violate lepton number. In all considered processes Majorana neutrinos were virtual, so LNV depends strongly on coherent effects connected with neutrino decay widths, CP phases, the nondegeneracy of heavy Majorana neutrino masses, and their mixings. That is why more refined LHC exclusion studies are highly desirable. Such an analysis could start from taking into account CP parities and a flavor mixing of two heavy neutrinos, as we sketched here. Furthermore, as there is a strong connection between high- and low-energy experiments, progress in many different intensity-frontier and neutrino oscillation experiments is highly welcome. For instance, the determination of the light neutrino parameters, including normal or inverted neutrino mass hierarchies, affects $(\beta\beta)_{0\nu}$ half-life predictions, which in turn influence heavy neutrino collider physics. The reasoning can be equally well reversed: high-energy collider processes give limits on the heavy sector of a given theory, which can in turn improve predictions for low-energy signals.

ACKNOWLEDGMENTS

We would like to thank Marek Zrałek and Marek Gluza for useful comments. Work is supported by the Polish National Science Centre (NCN), Grant No. DEC-2013/11/B/ST2/04023. R. S. is supported by the Natural Sciences and Engineering Research Council (NSERC) of Canada.

APPENDIX A: MAJORANA NEUTRINOS AND THE HIGH-ENERGY PROCESSES

We give several remarks related to the $pp \to W_2 \to N_a l \to lljj$ process, which is useful for interpreting experimental data. We use the following notation:

$$\sigma_{ij}^{\pm\pm} = \sigma(pp \to l_i^{\pm} l_j^{\pm} jj), \tag{A1}$$

$$\sigma_{ij}^{\pm\mp} = \sigma(pp \to l_i^{\pm} l_j^{\mp} jj), \tag{A2}$$

and collectively denote all of these cross sections by σ_{ij}. Here LNV is present when final dileptons have the same charge. Sometimes lepton charge (lepton number) is defined for each lepton family separately, N_e, N_μ, N_τ, (see, e.g., Ref. [50]). Then the lepton number is violated, for instance, in the $\mu^{\pm} \to e^{\pm}\gamma$ process. However, instead of LNV, it is often called CLFV. So, for $i \neq j$, the process (8) breaks both lepton and flavor numbers (LNV, CLFV), while the process (9) breaks flavor number (CLFV). In the SM, possible CLFV effects are completely negligible due to the smallness of active neutrino masses. (Commonly, we call light neutrinos *active* as opposed to *sterile* or *heavy* neutrinos.) Substantial effects may arise only if nonstandard heavy neutrinos exist.

In the original paper [28] on the heavy Majorana neutrino contribution to $pp \to lljj$, heavy neutrino mixings were assumed to be very small, suppressing the CLFV $\mu \to e\gamma$ process. Effectively, Majorana neutrinos with a trivial diagonal K_R were assumed. Moreover, due to $\Gamma_a/M_a \ll 1$, a simple factorization of the process into W_2 production times branching ratios is possible. Then, of course, the number of same-sign $eejj$ events is equal to the number of opposite-sign $eejj$ events, as in the case $r = 1$ in Fig. 4. However, in general the process depends on mixing of Majorana states, decay widths, CP phases, Majorana heavy neutrino mass splittings, the right-handed gauge boson mass, and its gauge coupling $\tilde{g}$. We found it worthwhile to revisit this case, especially since recently the $pp \to lljj$ process was studied by CMS in Ref. [47]. CMS reported 13 electron-positron-jet-jet (e^+e^-jj) events which are above the SM background, and one event which breaks the lepton number was identified (e^+e^+jj), so definitely $r \ll 1$. The CMS report triggered a lot of theoretical activity and was a fruitful seed for new ideas in the quest for NP at the LHC [46,54–93]. For earlier studies on $pp \to lljj$ see Refs. [32,35,39,49,94–106], and for more on heavy neutrino physics see, for instance, Refs. [19,20,50,107] and Refs. [26,94,97,103,108–129].

Let us note that the ATLAS Collaboration in the LHC Run 1 [130] only analyzed the possibility of Majorana neutrino detection (the search for SS dilepton final signals), so the possibility for an OS dilepton excess has been missed. As similar situations can appear in future experiments, it is therefore wise to know how far we can go with

heavy neutrinos and right-handed current physics in interpretations of possible signals, and how to effectively parametrize cross sections. For an initial discussion, see Ref. [56].

First, let us enumerate quantities which σ_{ij} depend on. The relevant electroweak dimensionless parameters are the gauge couplings $\tilde{g}$ (and g) and the neutrino mixing matrix K_R. On the other hand, the mass scales which are important for the process are M_{W_2}, M_a, and $\sqrt{s}$.

We shall discuss two setups in which it is possible to factor out the dependence on the mixing matrix K_R from the dependence on the above-mentioned scales. In the following we focus on the scenario in which all heavy neutrinos are lighter than W_2. In such a case one can estimate the magnitude of the decay widths of W_2 and N_a, and Γ_{W_2} and Γ_a, respectively:

$$\frac{\Gamma_{W_2}}{M_{W_2}} = \frac{\tilde{g}^2}{96\pi}\left(\sum_a F_W(x_a) + 18\right) \sim 10^{-2}, \tag{A3}$$

$$\frac{\Gamma_a}{M_a} = \frac{9\tilde{g}^4}{1024\pi^3} F(x_a) \sim 10^{-5}, \tag{A4}$$

where $x_a = M_a^2/M_{W_2}^2$, while $F_W(x)$ and $F(x)$ are the kinematical functions

$$F_W(x) = (2 - 3x + x^3)\theta(1-x), \tag{A5}$$

$$F(x) = \frac{12}{x}\left[1 - \frac{x}{2} - \frac{x^2}{6} + \frac{1-x}{x}\ln(1-x)\right]. \tag{A6}$$

In both cases $\Gamma/M \ll 1$. The narrow width approximation is valid in the region in which $M_{W_2} > M_{N_i}$ and M_{W_2} is not close to M_{N_i} or $\sqrt{s}$ [where the distance is measured in $\Gamma(W_2)$ units]. It turns out that when the mass splittings $M_a - M_b$, $a \neq b$ between heavy neutrinos are much different than Γ_a, one can express σ_{ij} as a product of two terms: one which depends only on the mixing matrix K_R, and one which depends on the remaining variables, i.e., $\tilde{g}$, $f(x, Q^2)$, $\sqrt{s}$, M_{W_2}, and $x_a = M_a^2/M_{W_2}^2$. We shall discuss two cases.

(a) Nondegenerate heavy neutrinos: $\min_{a\neq b}|M_a - M_b| \gg \max_a \Gamma_a$.
(b) Degenerate heavy neutrinos: $\max_{a\neq b}|M_a - M_b| \ll \min_a \Gamma_a$.

1. Case (a)

In this case interferences between different diagrams are negligible. One can factor out the dependence on the mixing matrix K_R in the following way:

$$\sigma_{ij}^{\pm\pm} = \sum_a \hat{\sigma}_a^{\pm\pm} |(K_R^\dagger)_{ia}(K_R^*)_{aj}|^2 + \text{INT}, \tag{A7}$$

$$\sigma_{ij}^{\pm\mp} = \sum_a \hat{\sigma}_a^{\pm\mp} |(K_R^\dagger)_{ia}(K_R)_{aj}|^2 + \text{INT}, \tag{A8}$$

where INT stands for small interference terms, while $\hat{\sigma}_a^{\pm\pm}$, $\hat{\sigma}_a^{\pm\mp}$ are "bare" cross sections calculated for $(K_R)_{aj} = \delta_{aj}$. Obviously, they depend only on $\tilde{g}$, $\sqrt{s}$, M_{W_2}, x_a but not on K_R. Due to $\Gamma_a \ll M_a$, such a "bare" cross section can be approximated by

$$\hat{\sigma}_a^{\pm\pm} = \sigma(pp \to W_2^\pm) \times \text{BR}(W_2^\pm \to N_a l_1^\pm)\text{BR}(N_a \to l_1^\pm jj), \tag{A9}$$

$$\hat{\sigma}_a^{+-} = [\sigma(pp \to W_2^+) + \sigma(pp \to W_2^-)] \times \text{BR}(W_2^+ \to N_a l_1^+)\text{BR}(N_a \to l_1^- jj). \tag{A10}$$

By direct computation one can check that Eqs. (A9) and (A10) lead to the following prediction for the ratio of the number of same-sign events (N_{SS}) to the number of opposite-sign events (N_{OS}):

$$r_{ij} = \left(\frac{N_{\text{SS}}}{N_{\text{OS}}}\right)_{ij} = \frac{\sigma_{ij}^{++} + \sigma_{ij}^{--}}{\sigma_{ij}^{+-}} \approx 1, \tag{A11}$$

regardless of the form of $(K_R)_{aj}$. An example of such behavior of r_{ij} is presented in Fig. 4 the main text. In that plot, the horizontal line corresponds to the value r_{ee} in the scenario when the splitting between the masses of N_1 and N_3 is about 1 GeV while $\Gamma_a \sim 1$ MeV.

2. Case (b)

In this case interferences are very important as they heavily influence the cross section. We consider a setup in which all three heavy neutrinos have the same mass. Analogously to case (a), it is convenient to factor out the dependence on the mixing matrix K_R:

$$\sigma_{ij}^{\pm\pm} = \hat{\sigma}^{\pm\pm}\left|\sum_a (K_R^\dagger)_{ia}(K_R^*)_{aj}\right|^2, \tag{A12}$$

$$\sigma_{ij}^{\pm\mp} = \hat{\sigma}^{\pm\mp}\left|\sum_a (K_R^\dagger)_{ia}(K_R)_{aj}\right|^2. \tag{A13}$$

Let us note that when K_R is unitary, $\sigma_{ij}^{\pm\mp} = \hat{\sigma}^{\pm\mp}\delta_{ij}$. $\hat{\sigma}$ are cross sections calculated for $(K_R)_{aj} = \delta_{aj}$. Due to $\Gamma_a \ll M_a$ the "bare" cross sections $\hat{\sigma}^{\pm\pm}$ and $\hat{\sigma}^{\pm\mp}$ can be approximated by

$$\hat{\sigma}^{\pm\pm} = \sigma(pp \to W_2^\pm) \times \text{BR}(W_2^\pm \to N_1 l_1^\pm)\text{BR}(N_1 \to l_1^\pm jj), \tag{A14}$$

$$\hat{\sigma}^{+-} = [\sigma(pp \to W_2^+) + \sigma(pp \to W_2^-)] \times \text{BR}(W_2^+ \to N_1 l_1^+)\text{BR}(N_1 \to l_1^- jj), \tag{A15}$$

which leads to

$$r_{ij} = \frac{\sigma_{ij}^{++} + \sigma_{ij}^{--}}{\sigma_{ij}^{+-}} \approx \left| \sum_a (K_R^\dagger)_{ia} (K_R^*)_{aj} \right|^2 . \qquad \text{(A16)}$$

When K_R is unitary one obtains $r_{ij} \leq 1$.

The results shown in Fig. 4 and the vanishing of the r dependence for heavy Majorana mass splittings can be understood as follows. The LHC kinematics and masses of particles allows for the exchange of a neutrino close to its mass shell. Then the total cross section is dominated by the exchange of the neutrino in the s channel. Close to the mass pole, the neutrino propagator can be described by the relativistic Breit-Wigner distribution. If we consider mixing between neutrino states, amplitudes corresponding to different mass eigenstates have to be added coherently. The interference between amplitudes corresponding to different mass eigenstates can be destructive, leading to a suppression of the SS lepton production cross section.

The size of the interference term can compete with the resonant contribution of the squared amplitudes only if the neutrino mass difference is of the order of the neutrino widths. These kinds of effects have been considered already in a model without right-handed currents in Ref. [27]. In our case the neutrino decay width is naturally very small, at the MeV level, and large interferences are possible; see the line r_0 in Fig. 4. Otherwise, the interference term contributes only to the continuum background and is negligible for the considered process (line r_1). Therefore, a suppression of the SS signal occurs only if the heavy Majorana neutrinos are (almost) degenerate.

In our numerical analysis, scalar decay modes of heavy neutrinos are negligible (heavy neutrino masses are smaller than heavy scalar masses) and the decay mode $N \to e^\pm W_1^\mp$ is dominant. For a discussion of possible decay-mode scenarios of heavy neutrinos, see, for instance, Ref. [131] (minimal left-right model) and Refs. [26,27] (models with heavy neutrino singlets).

We can also think about a situation where a process is t-channel dominated. In the t channel, neutrino propagators are far from their poles. Here interferences can be substantial even for very large Majorana neutrino mass splittings compared to decay widths because the signal is not dominated by the resonant contribution. Each neutrino propagator is a slowly varying function of energy and mass. Large interference effects can effectively lead to LNC (destructive interference may totally suppress the cross section). This can happen for another variant of the diagram shown in the dashed box of Fig. 1, namely, $e^-e^- \to W_2^- W_2^-$ [126,127,132–135]. The numerical results are shown in Fig. 5. The θ_{13} asymmetry for the cross section and a shift in the minimum is due to different weights in the amplitudes of N_1 and N_3.

This example is of pedagogical value as W_2, which is taken to be 1.4 TeV, is well below the present LHC direct limit, which is about 3 TeV. However, note that this strict LHC limit is based on a nondegenerate and no-mixing heavy neutrino scenario (for consequences, see Fig. 3 and the discussion in the main text). The point is that a relatively large cross section can be obtained only for on-shell W_2 pair production, and foreseen lepton collider center-of-mass energies are at most at the 3 TeV level. Heavier off-shell W_2 pair production would require very high luminosities for a detection of this signal as the cross section quickly drops below $\mathcal{O}(1)$ fb with increasing W_2 mass.

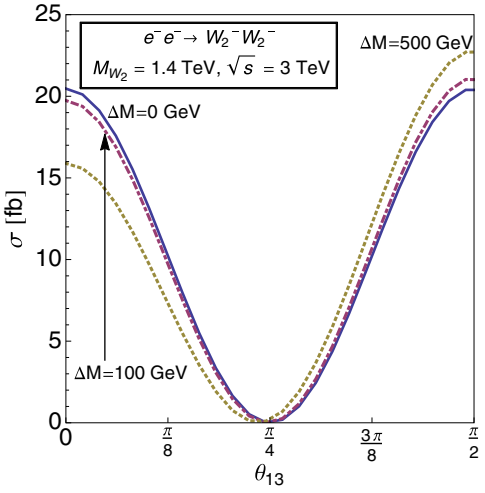

FIG. 5. Interference effects in the $e^-e^- \to W_2^- W_2^-$ LNV process for three different splittings $\Delta M = 0$, 100, and 500 GeV between masses of heavy neutrinos $N_{1,3}$. $M_{W_2} = 1.4$ TeV, $\sqrt{s} = 3$ TeV, $M_{1,3} = 1$ TeV $\pm \Delta M/2$, $M_2 = 10$ TeV, K_R is given as in Eq. (6), and $\phi_3 = \pi/2$.

APPENDIX B: LOW-ENERGY CLFV PROCESSES

In the SM the CLFV effects are negligible due to the small masses of light, active neutrinos [136]. Similarly to the $pp \to lljj$ process, for substantial effects new heavy particles are needed. The best limits have been obtained so far in the muon-electron sector, though nowadays processes involving the tau leptons also start to play a role. Present and planned limits for the most important low-energy CLFV processes are gathered in Table II.

TABLE II. Current and planned limits on the CLFV branching ratios [137–140]. For the muon coherent conversion process $\mu N \to eN$ the limit is given as a ratio of the conversion rate to the muon nuclear capture $\mu N \to \nu_\mu N'$ rate.

Process	Current Limit	Planned Limit
$\tau \to \mu\gamma$	4.4×10^{-8}	3.0×10^{-9}
$\tau \to e\gamma$	3.3×10^{-8}	3.0×10^{-9}
$\tau \to \mu\mu\mu$	2.1×10^{-8}	1.0×10^{-9}
$\tau \to eee$	2.7×10^{-8}	1.0×10^{-9}
$\mu \to e\gamma$	5.7×10^{-13}	6.0×10^{-14}
$\mu \to eee$	1.0×10^{-12}	1.0×10^{-16}
$\mu N \to eN$	7.0×10^{-13}	1.0×10^{-17}

Our choice of the mixing matrix (6) implies that a mixing is present only between taus and electrons in the discussed model. Let us consider the CLFV process $l \to l'\gamma$; in our case we are interested in an estimation of the nonzero $\tau \to e\gamma$ branching ratio. The main contribution to this process comes from the diagram containing virtual heavy neutrinos. The branching ratio for the general case $l \to l'\gamma$ [141], adopted to our case and including right-handed currents, is

$$\mathrm{BR}(l \to l'\gamma) \approx \frac{3}{8}\frac{\alpha}{\pi}\left(\frac{\tilde{g}}{g}\frac{M_{W_1}}{M_{W_2}}\right)^4 \times \left|\sum_a (K_R^\dagger)_{l'a}(K_R)_{al} F\left(\frac{M_a^2}{M_{W_2}^2}\right)\right|^2, \quad \text{(B1)}$$

where M_a is the mass of the heavy neutrino and

$$F(x) = \frac{10 - 43x + 78x^2 - 49x^3 + 4x^4 + 18x^3 \ln x}{6(1-x)^4}. \quad \text{(B2)}$$

For unitary K_R we can add any constant to the function $F(x)$ without affecting the branching ratio. It is convenient to define a new function $\phi(x)$ such that $\phi(0) = 0$. This can be obtained by the redefinition

$$F(x) \to \phi(x) = F(x) - F(0) = -\frac{x[1 - 6x + 3x^2 + 2x^3 - 6x^2 \ln(x)]}{2(1-x)^4}. \quad \text{(B3)}$$

In this instance we recover the classical result [142], which is valid only for the unitary mixing matrix, but for any mass ratio of the neutrinos and vector bosons. The function $\phi(x)$ is monotonically increasing and bounded in the physical domain, $0 \le \phi(x) < 1$ for $0 \le x < \infty$. This allows us to derive an upper bound on the branching ratio in the case of mixing between two generations,

$$\mathrm{BR}(l \to l'\gamma) < \frac{3}{8}\frac{\alpha}{\pi}\left(\frac{\tilde{g}}{g}\frac{M_{W_1}}{M_{W_2}}\right)^4 (\sin\theta_{13}\cos\theta_{13})^2 \le \frac{3}{32}\frac{\alpha}{\pi}\left(\frac{\tilde{g}}{g}\frac{M_{W_1}}{M_{W_2}}\right)^4. \quad \text{(B4)}$$

For completeness, let us also recall the formula for $M_a/M_{W_2} \ll 1$. In this case, Eq. (B2) can be further simplified,

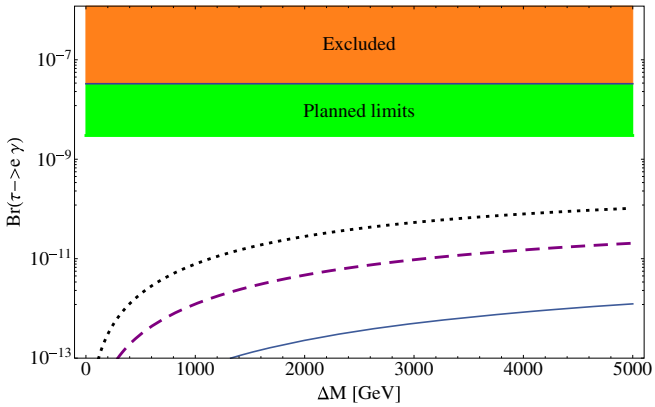

FIG. 6. $\tau \to e\gamma$ branching ratio as a function of mass splitting $\Delta M = M_3 - M_1$. The mixing between the first and third generations is assumed to be maximal. We chose $M_{W_2} = 2.2$ TeV (dotted line), $M_{W_2} = 3$ TeV (dashed line), and $M_{W_2} = 5$ TeV (solid line). Also, $M_1 = M_{W_2}/2$.

$$\mathrm{BR}(l \to l'\gamma) = \frac{3\alpha}{32\pi}\left(\frac{\tilde{g}}{g}\frac{M_{W_1}}{M_{W_2}}\right)^4 \left(\sin\theta_{13}\cos\theta_{13}\frac{\Delta m_{12}^2}{M_{W_2}^2}\right)^2. \quad \text{(B5)}$$

For $M_{W_2} = 2.2$ TeV and $g = \tilde{g}$ the branching ratio is suppressed by $(3\alpha/32\pi) \times (M_{W_1}/M_{W_2})^4 \sim 4 \times 10^{-10}$. It gives a good estimation of the order of magnitude of the CLFV effect. To investigate it more carefully we chose the maximal mixing $\theta_{13} = \pi/4$ and a large mass difference between N_1 and N_3. (Note that for a unitary K_R the contribution does not depend directly on the absolute values of the masses of neutrinos, but rather on their difference, just as it is in the case of light neutrinos.)

In Fig. 6 the branching ratio $\tau \to e\gamma$ is plotted for the maximal mixing between the first and third generations. We assume $M_1 = M_{W_2}/2$ and we vary M_3. Different lines correspond to M_{W_2} equal to 2.2, 3, and 5 TeV.

We can see that the K_R parametrization for the effective mixture of two heavy Majorana neutrinos given in Eq. (6) fulfills the relevant CLFV limits. It is instructive to notice that even if the planned limit would improve further by an order of magnitude, we would be able to probe only the large mass splittings at the TeV level.

APPENDIX C: RELATIONS AMONG HEAVY NEUTRINO MASSES, *CP* PHASES, AND MIXING MATRIX ELEMENTS

Complex couplings in interactions and complex elements of mass matrices may lead to *CP*-violating effects. Gauge transformations and unitary transformations on fields may reduce the number of *CP* phases [50,143]. To see which mass matrix leads to degenerate neutrino masses and to the mixing matrix K_R discussed in the main text, it is enough to consider the two-neutrino case [N_2 does

not mix in Eq. (6)]. Studying this case in detail, the connection between CP parities and mass eigenvalues can also be seen.

Let us start from a general 2×2 complex symmetric mass matrix (the symmetry of the matrix comes from Hermitian-conjugated mass terms)

$$M=\begin{pmatrix} ae^{i\alpha} & be^{i\beta} \\ be^{i\beta} & ce^{i\gamma}\end{pmatrix}. \tag{C1}$$

In general it can be diagonalized using biunitary matrices. However, taking $M^\dagger M$, a Hermitian matrix emerges which can be diagonalized using a single unitary matrix V,

$$V^\dagger(M^\dagger M)V=\mathrm{diag}(m_1^2,m_2^2), \tag{C2}$$

$$m_{1,2}^2=\frac{1}{2}\left[a^2+c^2+2b^2\pm\sqrt{(a^2-c^2)^2+\Omega}\right], \tag{C3}$$

$$\Omega=4b^2[a^2+c^2+2ac\cos(\alpha+\gamma-2\beta)]. \tag{C4}$$

We can see that $m_1=m_2$ if $a=\pm c$ and $\alpha+\gamma-2\beta=\pi$ (so the element b can take any value).

In general, squared eigenvalues in Eq. (C3) are still complex, so we assume that for the same matrix V,

$$V^TMV=\begin{pmatrix} m_1e^{-2i\phi_1} & 0 \\ 0 & m_2e^{-2i\phi_2}\end{pmatrix}\equiv\begin{pmatrix} m_1\rho_1 & 0 \\ 0 & m_2\rho_2\end{pmatrix}, \tag{C5}$$

where $m_{1,2}\geq 0$, $m_{1,2}\in\mathbb{R}$, and $\rho_{1,2}=\pm 1$. Note that the Hermitian conjugation of V in Eq. (C2) has been replaced by transposition as $(M^\dagger M)^*=M^\dagger M$.

Absorbing phases into V, we get $U=V\mathrm{diag}(e^{i\phi_1},e^{i\phi_2})$. Taking V leads to the squared eigenvalues in a following form:

$$V=\begin{pmatrix} \cos\xi & \sin\xi \\ -e^{i\delta}\sin\xi & e^{i\delta}\cos\xi\end{pmatrix}, \tag{C6}$$

where ξ and δ are fixed through the Eq. (C2),

$$\tan 2\xi=\frac{2|abe^{i(\alpha-\beta)}+bce^{i(\beta-\gamma)}|}{c^2-a^2}, \tag{C7}$$

$$e^{i\delta}=\frac{abe^{i(\alpha-\beta)}+bce^{i(\beta-\gamma)}}{|abe^{i(\alpha-\beta)}+bce^{i(\beta-\gamma)}|}. \tag{C8}$$

We arrive at a general form of the unitary matrix U which diagonalizes M and gives positive eigenvalues [$s_\xi\equiv\sin\xi$, $c_\xi\equiv\cos\xi$],

$$U=\begin{pmatrix} c_\xi e^{i\phi_1} & s_\xi e^{i\phi_2} \\ -s_\xi e^{i(\delta+\phi_1)} & c_\xi e^{i(\delta+\phi_2)}\end{pmatrix}, \tag{C9}$$

$$e^{-2i\phi_1}=\frac{ac_\xi^2e^{i\alpha}-cs_\xi^2e^{i(\gamma+2\delta)}}{m_1\cos 2\xi}, \tag{C10}$$

$$e^{-2i\phi_2}=\frac{cc_\xi^2e^{i(\gamma+2\delta)}-as_\xi^2e^{i\alpha}}{m_2\cos 2\xi}. \tag{C11}$$

The phases $\phi_{1,2}$ are fixed by solving the relation $U^TMU=\mathrm{diag}(m_1,m_2)$.

Let us assume a real matrix M, with $\alpha=\beta=\gamma=0$, $a>0$, $b>0$, $c<0$. Such a matrix has one positive and one negative, real eigenvalue. By assigning $\rho_1<0$ and $\rho_2>0$, we have $\phi_1=\pm\pi/2$, $\phi_2=0$:

$$U=\begin{pmatrix} ic_\xi & s_\xi \\ -is_\xi & c_\xi\end{pmatrix}, \tag{C12}$$

which corresponds, up to transposition, to the mixing matrix K_R between N_1 and N_3 states in Eq. (6) (with $\phi_3=\pi/2$). In addition, for $a=-c$, $|m_1|=|m_2|$ (as already shown before).

We can see that the first column in Eq. (C12) is just multiplied by i. It is connected with CP parities of neutrinos. To establish this relation, the interaction term (2) must also be studied. Let us first note that for degenerate N_a states there is some symmetry in the mass term, as $M\sim N^TN$, e.g., for our two-dimensional case we have

$$\begin{pmatrix} N_1 \\ N_2\end{pmatrix}=\begin{pmatrix} \cos\alpha & -\sin\alpha \\ \sin\alpha & \cos\alpha\end{pmatrix}\begin{pmatrix} N_1' \\ N_2'\end{pmatrix}. \tag{C13}$$

We demand that the Lagrangian (2) expressed through prime fields differs from its original by the phase factor $e^{\pm i\alpha}$, which can be absorbed later on; schematically,

$$\mathcal{L}\sim[\overline{N}_1(U^T)_{1a}+\overline{N}_2(U^T)_{2a}]l_b \tag{C14}$$

$$=\overline{N}_1{}'[\cos\alpha(U^T)_{1a}+\sin\alpha(U^T)_{2a}]l_b \tag{C15}$$

$$+\overline{N}_2'[-\sin\alpha(U^T)_{1a}+\cos\alpha(U^T)_{2a}]l_b. \tag{C16}$$

Now, if $(U^T)_{1a}=\pm i(U^T)_{2a}$,

$$\mathcal{L}\sim e^{\pm i\alpha}\left(\frac{\overline{N}_1'\pm i\overline{N}_2'}{\sqrt{2}}\right)\sqrt{2}(U^T)_{2a}l_b \tag{C17}$$

$$\equiv\Phi_D(U^T)'_{2a}, \tag{C18}$$

where $\Phi_D\equiv e^{\pm i\alpha}(\overline{N}_1'\pm i\overline{N}_2')/\sqrt{2}$ and $(U^T)'_{2a}\equiv\sqrt{2}(U^T)_{2a}$.

As we can see, invariance of the Lagrangian for two Majorana neutrinos with α symmetry implies a Dirac neutrino. It remains to show that these two Majorana neutrinos have opposite CP parities. Imaginary elements of the matrix (C9) will affect any terms in the Lagrangian that are linear in N_1. Those terms under CP symmetry will change the sign, leading to apparent maximal CP violation. However, we can also change the CP phase of the neutrino field N_2. CP conservation can be restored if the field transforms as $N_1 \to -N_1$. More generally, if $N_1 \to \eta_{CP} N_1$, then $N_2 \to -\eta_{CP} N_2$ [144]. With these transformation properties our theory is CP conserving and, as expected, both Majorana fields have opposite CP parities.

This is a general situation. For the CP-conserving case, the neutrino N_1 with a negative-mass eigenvalue has opposite CP parity as neutrino N_2 with a positive-mass eigenvalue, $-\eta_{CP}(N_1) = \eta_{CP}(N_2) = i$ [50]. In such a case, the corresponding columns in the mixing matrix (C12) are purely real or complex.

It is worth mentioning that nontrivial mixing angles, such as θ_{13} in K_R [Eq. (6)], have a physical meaning for degenerate neutrinos only if the CP parities of neutrinos are different (in other words, the mixing matrix cannot be real). First, let us consider some process regardless of the nature of neutrinos. In this case, the unitarity of K_R and the degeneracy of the neutrino masses makes the rate for this process independent of the mixing angle. This is observed for all LNC processes, like $\mu \to e\gamma$ or $W_2^- \to e^- \overline{N}_a$. On the other hand, if some process is permitted only for Majorana neutrinos then the dependence on the mixing angle can appear only if the Majorana phase is nonzero. This Majorana process usually involves a charge-conjugation operator and its amplitude depends on elements of the matrix $K_R K_R^T$. A typical example is the double neutrinoless beta decay. For neutrinos with different CP parities this matrix is not unity and can have a nontrivial dependence on the mixing angle. However, if K_R is real, i.e., orthogonal, the neutrinos have equal CP parities and cannot be distinguished. For the corresponding $pp \to lljj$ cases, see Eqs. (A12) and (A13).

APPENDIX D: SWINGING BETWEEN DIRAC AND MAJORANA STATES: NEUTRINO MASS MATRICES

In Ref. [145] more historical remarks can be found on Weyl, Dirac, and Majorana neutrinos. Here we focus on neutrino mass matrices as the actual composition of neutrino states and their nature stems from them.

There are many mechanisms for neutrino mass generation. Typically, these are radiative mass generations or tree-level (effective) constructions; in both cases, nonstandard fields, interactions, or symmetries are necessarily involved.

By ranging neutrino masses from zero to $M_i \geq 10^9$ GeV, mass mechanisms introduce different neutrino states [21]. Apart from Dirac or Majorana types, there are pseudo-Dirac (or quasi-Dirac) [9], schizophrenic [146], or vanilla [106] neutrinos, to name some of them. Popular seesaw mechanisms give a possibility for a dynamical explanation of why the known active neutrino states are so light. They appear to be of Majorana type (recently, a dynamical explanation for Dirac light neutrinos was proposed [147]). Seesaw type-I, -II, and -III models have been worked out in Refs. [10,12, 148,149], Ref. [150], and Ref. [151], respectively. A hybrid mechanism is also possible [152]. For the original inverse seesaw see Refs. [17,18], and for its generalizations see Refs. [55,153–156].

Here we recap the classical type-I seesaw, and the more universal (but at the same time more complex) inverse seesaw mechanism. For the seesaw type-I mass matrix and SM leptonic (L) and scalar $\tilde{\phi}$ fields we have

$$\mathcal{L}_{\mathrm{Y}} = -Y_{ij} \overline{L'_{iL}} N'_{jR} \tilde{\phi} + \mathrm{H.c.}, \tag{D1}$$

$$\mathcal{L}_{\mathrm{M}} = -\frac{1}{2} M_{ij} \overline{N'_{iL}} N'_{jR} + \mathrm{H.c.}, \tag{D2}$$

$$\mathcal{L}_{\mathrm{Y}} + \mathcal{L}_{\mathrm{M}} == -\frac{1}{2} (\overline{\nu}'_L \overline{N}'_L) \begin{pmatrix} 0 & \frac{v}{\sqrt{2}} Y \\ \frac{v}{\sqrt{2}} Y^T & M \end{pmatrix} \begin{pmatrix} \nu'_R \\ N'_R \end{pmatrix}. \tag{D3}$$

If the indices i, j run from 1 to 3, we have in general a 6×6 mass matrix. For the above, the neutrino mass matrix can be identified with Dirac M_D and Majorana M_R mass terms,

$$M_\nu = \begin{pmatrix} 0 & M_D \\ M_D^T & M_R(v_R) \end{pmatrix}. \tag{D4}$$

With $M_D \ll M_R$,

$$m_N \sim M_R, \tag{D5}$$

$$m_{\mathrm{light}} \sim M_D^2 / M_R. \tag{D6}$$

For $M_D \sim \mathcal{O}(1)$ GeV and demanding light neutrino masses of the order of 0.1 eV, without artificial fine-tunings we get the heavy Majorana mass scale $M_R \sim 10^{15}$ GeV.

As typically $M_D[\mathcal{O}(\mathrm{MeV})] \ll M_R[\mathcal{O}(\mathrm{TeV})]$, most of possible connections between heavy N and light ν neutrino sectors are cut away, and we can explore heavy-sector effects exclusively, as is done in Eq. (6). In this case the neutrino mixing matrix takes the following form:

$$U \approx \begin{pmatrix} U_{\mathrm{PMNS}} & 0 \\ 0 & K_R^\dagger \end{pmatrix}, \tag{D7}$$

where K_R is a unitary 3×3 matrix defined by $M_R = K_R^T \mathrm{diag}(M_1, M_2, M_3) K_R$, $M_a > 0$.

A more universal neutrino mass construction is connected with the so-called inverse or linear seesaw mechanism. Classically, the pseudo-Dirac neutrino has been introduced for light neutrinos demanding $m_D \gg m_R$ in Eq. (D4). In such a case neutrinos can mix maximally, leading to the almost degenerate mass states with opposite CP phases [50].

In the inverse seesaw the neutrino ranges from the pure Majorana case, to the pseudo-Dirac scenario, and to the pure Dirac scenario. Also, relatively large light-heavy neutrino mixings can be obtained here [17,49,54]. This means that in the main text we mainly explore the type-I seesaw scenarios, Eq. (D7).

In the original inverse seesaw proposal, the lepton number violation is small, being directly proportional to the light neutrino masses.

The generalized inverse seesaw neutrino mass matrix in the extended flavor basis $\{\nu^C, N, S^C\}$ is given by

$$\mathcal{M} = \begin{pmatrix} 0 & M_D & 0 \\ M_D^{\mathsf{T}} & \mu_R & M_N^{\mathsf{T}} \\ 0 & M_N & \mu_S \end{pmatrix}, \tag{D8}$$

with two eigenvalues, which are

$$M_{N_{1,2}} \simeq \frac{1}{2}\left[\mu_R \pm \sqrt{\mu_R^2 + 4M_N^2}\right]. \tag{D9}$$

For $\mu_R \ll M_N$, $N_{1,2}$, a pseudo-Dirac pair emerges. For $\mu_R \gg M_N$, N_1, a purely Majorana state with $M_1 = \mu_R$ is realized.

Thus, for intermediate values of μ_R, we can have scenarios with a varying degree of lepton number breaking [17,101,116,130,157].

In the inverse seesaw case, since there are two pairs of SM singlet fermions, they can always form Dirac pairs in the limit of small LNV. However, in the type-I seesaw with three Majorana neutrinos, we can get one Dirac and one unpaired Majorana neutrino, as in the case of Eq. (5).

In the context of the considered models and phenomenological studies, let us focus on the r parameter in the $pp \to lljj$ process. The following question naturally emerges: is it possible to establish whether we have a pure Dirac state or a Majorana composition? In the setup discussed in this work, the lepton number conservation is realized ($r = 0$) only when two heavy Majorana neutrinos are degenerate and have opposite parities, or equivalently, the heavy neutrino is of the Dirac type. But, there is no possibility to measure $r = 0$ exactly. The best that can be done is to derive more and more precise bounds on r. In turn, such bounds on the lepton number violation provide limits on the mass splittings and mixing parameters of heavy Majorana neutrinos.

One should also keep in mind that in more complicated scenarios $r = 0$ can also be realized when masses of heavy neutrinos are not degenerate. For example, effective operators which violate the lepton number may be present in the model. Then, contributions to $pp \to lljj$ coming from heavy neutrinos and those coming from an additional sector of the theory may interfere and lead to $r = 0$. It is clear that such a configuration would require severe fine-tuning of the model parameters.

[1] J. N. Bahcall and R. Davis, Science **191**, 264 (1976).
[2] Y. Fukuda *et al.* (Super-Kamiokande Collaboration), Phys. Rev. Lett. **81**, 1562 (1998).
[3] Q. R. Ahmad *et al.* (SNO Collaboration), Phys. Rev. Lett. **89**, 011301 (2002).
[4] F. E. Wietfeldt and E. B. Norman, Phys. Rep. **273**, 149 (1996).
[5] A. Franklin, Rev. Mod. Phys. **67**, 457 (1995).
[6] T. Adam *et al.* (OPERA Collaboration), J. High Energy Phys. 10 (2012) 093.
[7] M. Antonello *et al.* (ICARUS Collaboration), Phys. Lett. B **713**, 17 (2012).
[8] H. V. Klapdor-Kleingrothaus and I. V. Krivosheina, Mod. Phys. Lett. A **21**, 1547 (2006).
[9] E. Akhmedov, arXiv:1412.3320.
[10] P. Minkowski, Phys. Lett. B **67**, 421 (1977).
[11] T. Yanagida, Conf. Proc. **C7902131**, 95 (1979).
[12] M. Gell-Mann, P. Ramond, and R. Slansky, Conf. Proc. **C790927**, 315 (1979).
[13] R. N. Mohapatra and G. Senjanovic, Phys. Rev. Lett. **44**, 912 (1980).
[14] J. Schechter and J. W. F. Valle, Phys. Rev. D **25**, 774 (1982).
[15] W. Rodejohann, Int. J. Mod. Phys. E **20**, 1833 (2011).
[16] H. Pas and W. Rodejohann, New J. Phys. **17**, 115010 (2015).
[17] R. N. Mohapatra, Phys. Rev. Lett. **56**, 561 (1986).
[18] R. N. Mohapatra and J. W. F. Valle, Phys. Rev. D **34**, 1642 (1986).
[19] R. N. Mohapatra and P. B. Pal, *Massive Neutrinos in Physics and Astrophysics*, 3rd ed. (World Scientific, Singapore, 2004).
[20] C. Giunti and C. W. Kim, *Fundamentals of Neutrino Physics and Astrophysics* (Oxford University, New York, 2007).
[21] M. Drewes, Int. J. Mod. Phys. E **22**, 1330019 (2013).
[22] A. de Gouvea and P. Vogel, Prog. Part. Nucl. Phys. **71**, 75 (2013).

[23] Y. Kuno (COMET Collaboration), Prog. Theor. Exp. Phys. **2013**, 022C01 (2013).
[24] D. Brown (Mu2e Collaboration), Nucl. Part. Phys. Proc. **260**, 151 (2015).
[25] N. Abgrall *et al.* (Majorana Collaboration), Adv. High Energy Phys. **2014**, 365432 (2014).
[26] A. Pilaftsis, Z. Phys. C **55**, 275 (1992).
[27] S. Bray, J. S. Lee, and A. Pilaftsis, Nucl. Phys. **B786**, 95 (2007).
[28] W.-Y. Keung and G. Senjanovic, Phys. Rev. Lett. **50**, 1427 (1983).
[29] J. Gluza and M. Zrałek, Phys. Rev. D **45**, 1693 (1992).
[30] A. Denner, H. Eck, O. Hahn, and J. Kublbeck, Phys. Lett. B **291**, 278 (1992).
[31] M. Hirsch, H. V. Klapdor-Kleingrothaus, and O. Panella, Phys. Lett. B **374**, 7 (1996).
[32] V. Tello, M. Nemevsek, F. Nesti, G. Senjanovic, and F. Vissani, Phys. Rev. Lett. **106**, 151801 (2011).
[33] M. Mitra, G. Senjanovic, and F. Vissani, Nucl. Phys. **B856**, 26 (2012).
[34] A. Faessler, A. Meroni, S. T. Petcov, F. Simkovic, and J. Vergados, Phys. Rev. D **83**, 113003 (2011).
[35] M. Nemevsek, G. Senjanovic, and V. Tello, Phys. Rev. Lett. **110**, 151802 (2013).
[36] A. Meroni, S. T. Petcov, and F. Simkovic, J. High Energy Phys. 02 (2013) 025.
[37] J. Barry and W. Rodejohann, J. High Energy Phys. 09 (2013) 153.
[38] S. Pascoli, M. Mitra, and S. Wong, Phys. Rev. D **90**, 093005 (2014).
[39] C.-H. Lee, P. S. Bhupal Dev, and R. N. Mohapatra, Phys. Rev. D **88**, 093010 (2013).
[40] P. S. Bhupal Dev, S. Goswami, M. Mitra, and W. Rodejohann, Phys. Rev. D **88**, 091301 (2013).
[41] A. Meroni and E. Peinado, Phys. Rev. D **90**, 053002 (2014).
[42] A. Meroni, Eur. Phys. J. Plus **130**, 232 (2015).
[43] M. Czakon, J. Gluza, and M. Zrałek, Phys. Lett. B **465**, 211 (1999).
[44] V. D. Barger and K. Whisnant, Phys. Lett. B **456**, 194 (1999).
[45] Z.-z. Xing, Z.-h. Zhao, and Y.-L. Zhou, Eur. Phys. J. C **75**, 423 (2015).
[46] R. L. Awasthi, P. S. B. Dev, and M. Mitra, Phys. Rev. D **93**, 011701 (2016).
[47] V. Khachatryan *et al.* (CMS Collaboration), Eur. Phys. J. C **74**, 3149 (2014).
[48] J. Gluza, Acta Phys. Pol. B **33**, 1735 (2002).
[49] C.-Y. Chen, P. S. B. Dev, and R. Mohapatra, Phys. Rev. D **88**, 033014 (2013).
[50] S. M. Bilenky and S. T. Petcov, Rev. Mod. Phys. **59**, 671 (1987); **60**, 575(E) (1988).
[51] B. Kayser, Phys. Rev. D **30**, 1023 (1984).
[52] B. Kayser, F. Gibrat-Debu, and F. Perrier, World Sci. Lect. Notes Phys. **25**, 1 (1989).
[53] L. Baudis *et al.*, Phys. Rev. Lett. **83**, 41 (1999).
[54] F. F. Deppisch, L. Graf, S. Kulkarni, S. Patra, W. Rodejohann, N. Sahu, and U. Sarkar, Phys. Rev. D **93**, 013011 (2016).
[55] P. S. Bhupal Dev and R. N. Mohapatra, Phys. Rev. Lett. **115**, 181803 (2015).
[56] J. Gluza and T. Jeliński, Phys. Lett. B **748**, 125 (2015).
[57] F. F. Deppisch, T. E. Gonzalo, S. Patra, N. Sahu, and U. Sarkar, Phys. Rev. D **90**, 053014 (2014).
[58] M. Heikinheimo, M. Raidal, and C. Spethmann, Eur. Phys. J. C **74**, 3107 (2014).
[59] F. F. Deppisch, T. E. Gonzalo, S. Patra, N. Sahu, and U. Sarkar, Phys. Rev. D **91**, 015018 (2015).
[60] J. A. Aguilar-Saavedra and F. R. Joaquim, Phys. Rev. D **90**, 115010 (2014).
[61] J. C. Vasquez, J. High Energy Phys. 05 (2016) 176.
[62] G. Senjanovic and V. Tello, Phys. Rev. Lett. **114**, 071801 (2015).
[63] J. N. Ng, A. de la Puente, and B. W.-P. Pan, J. High Energy Phys. 12 (2015) 172.
[64] B. A. Dobrescu and Z. Liu, Phys. Rev. Lett. **115**, 211802 (2015).
[65] J. Brehmer, J. Hewett, J. Kopp, T. Rizzo, and J. Tattersall, J. High Energy Phys. 10 (2015) 182.
[66] J. C. Vasquez, J. High Energy Phys. 09 (2015) 131.
[67] P. Coloma, B. A. Dobrescu, and J. Lopez-Pavon, Phys. Rev. D **92**, 115023 (2015).
[68] A. Das, P. S. Bhupal Dev, and N. Okada, Phys. Lett. B **735**, 364 (2014).
[69] J. Berger, J. A. Dror, and W. H. Ng, J. High Energy Phys. 09 (2015) 156.
[70] B. A. Dobrescu and Z. Liu, J. High Energy Phys. 10 (2015) 118.
[71] J. Hisano, N. Nagata, and Y. Omura, Phys. Rev. D **92**, 055001 (2015).
[72] M. E. Krauss and W. Porod, Phys. Rev. D **92**, 055019 (2015).
[73] M. Dhuria, C. Hati, and U. Sarkar, Phys. Rev. D **93**, 015001 (2016).
[74] T. Bandyopadhyay, B. Brahmachari, and A. Raychaudhuri, J. High Energy Phys. 02 (2016) 023.
[75] P. S. B. Dev, D. Kim, and R. N. Mohapatra, J. High Energy Phys. 01 (2016) 118.
[76] F. F. Deppisch, Acta Phys. Pol. B **46**, 2301 (2015).
[77] F. F. Deppisch, P. S. Bhupal Dev, and A. Pilaftsis, New J. Phys. **17**, 075019 (2015).
[78] S. Banerjee, M. Mitra, and M. Spannowsky, Phys. Rev. D **92**, 055013 (2015).
[79] M. Dhuria, C. Hati, R. Rangarajan, and U. Sarkar, Phys. Rev. D **92**, 031701 (2015).
[80] T. Jeliński and M. Kordiaczyńska, Acta Phys. Pol. B **46**, 2193 (2015).
[81] P. Ko and T. Nomura, Phys. Lett. B **753**, 612 (2016).
[82] R. Leonardi, L. Alunni, F. Romeo, L. Fano, and O. Panella, arXiv:1510.07988.
[83] J. H. Collins and W. H. Ng, J. High Energy Phys. 01 (2016) 159.
[84] B. A. Dobrescu and P. J. Fox, J. High Energy Phys. 05 (2016) 047.
[85] C. Hati, G. Kumar, and N. Mahajan, J. High Energy Phys. 01 (2016) 117.
[86] U. Aydemir, Int. J. Mod. Phys. A **31**, 1650034 (2016).
[87] C. Garcia-Cely and J. Heeck, J. Cosmol. Astropart. Phys. 03 (2016) 021.
[88] R. Blumenhagen, J. High Energy Phys. 01 (2016) 039.
[89] A. Dasgupta, M. Mitra, and D. Borah, arXiv:1512.09202.

[90] J. Shu and J. Yepes, arXiv:1512.09310.
[91] C. Hati, Phys. Rev. D **93**, 075002 (2016).
[92] A. Das, N. Nagata, and N. Okada, J. High Energy Phys. 03 (2016) 049.
[93] J. Shu and J. Yepes, arXiv:1601.06891.
[94] A. Datta, M. Guchait, and A. Pilaftsis, Phys. Rev. D **50**, 3195 (1994).
[95] A. Ferrari, J. Collot, M.-L. Andrieux, B. Belhorma, P. de Saintignon, J.-Y. Hostachy, Ph. Martin, and M. Wielers, Phys. Rev. D **62**, 013001 (2000).
[96] J. Kersten and A. Y. Smirnov, Phys. Rev. D **76**, 073005 (2007).
[97] F. del Aguila, J. A. Aguilar-Saavedra, and R. Pittau, J. High Energy Phys. 10 (2007) 047.
[98] F. del Aguila and J. A. Aguilar-Saavedra, Phys. Lett. B **672**, 158 (2009).
[99] A. Maiezza, M. Nemevsek, F. Nesti, and G. Senjanovic, Phys. Rev. D **82**, 055022 (2010).
[100] M. Nemevsek, F. Nesti, G. Senjanovic, and Y. Zhang, Phys. Rev. D **83**, 115014 (2011).
[101] C.-Y. Chen and P. S. B. Dev, Phys. Rev. D **85**, 093018 (2012).
[102] S. Das, F. Deppisch, O. Kittel, and J. Valle, Phys. Rev. D **86**, 055006 (2012).
[103] J. Chakrabortty, J. Gluza, R. Sevillano, and R. Szafron, J. High Energy Phys. 07 (2012) 038.
[104] T. Han, I. Lewis, R. Ruiz, and Z.-g. Si, Phys. Rev. D **87**, 035011 (2013); **87**, 039906(E) (2013).
[105] J. A. Aguilar-Saavedra and F. R. Joaquim, Phys. Rev. D **86**, 073005 (2012).
[106] P. S. B. Dev and R. N. Mohapatra, arXiv:1308.2151.
[107] B. Kayser, Phys. Rev. D **26**, 1662 (1982).
[108] D. A. Dicus, D. D. Karatas, and P. Roy, Phys. Rev. D **44**, 2033 (1991).
[109] A. Datta and A. Pilaftsis, Phys. Lett. B **278**, 162 (1992).
[110] A. Datta, M. Guchait, and D. P. Roy, Phys. Rev. D **47**, 961 (1993).
[111] J. Gluza and M. Zrałek, Phys. Rev. D **48**, 5093 (1993).
[112] J. Gluza and M. Zrałek, Phys. Lett. B **372**, 259 (1996).
[113] J. Gluza, Phys. Lett. B **403**, 304 (1997).
[114] J. Gluza, J. Maalampi, M. Raidal, and M. Zrałek, Phys. Lett. B **407**, 45 (1997).
[115] F. del Aguila, J. A. Aguilar-Saavedra, A. Martinez de la Ossa, and D. Meloni, Phys. Lett. B **613**, 170 (2005).
[116] T. Han and B. Zhang, Phys. Rev. Lett. **97**, 171804 (2006).
[117] A. Atre, T. Han, S. Pascoli, and B. Zhang, J. High Energy Phys. 05 (2009) 030.
[118] A. Ibarra, E. Molinaro, and S. T. Petcov, J. High Energy Phys. 09 (2010) 108.
[119] R. Adhikari and A. Raychaudhuri, Phys. Rev. D **84**, 033002 (2011).
[120] C. G. Cely, A. Ibarra, E. Molinaro, and S. T. Petcov, Phys. Lett. B **718**, 957 (2013).
[121] P. S. Bhupal Dev, R. Franceschini, and R. N. Mohapatra, Phys. Rev. D **86**, 093010 (2012).
[122] A. Das and N. Okada, Phys. Rev. D **88**, 113001 (2013).
[123] P. S. B. Dev, A. Pilaftsis, and U.-K. Yang, Phys. Rev. Lett. **112**, 081801 (2014).
[124] J. C. Helo, M. Hirsch, and S. Kovalenko, Phys. Rev. D **89**, 073005 (2014).
[125] D. Alva, T. Han, and R. Ruiz, J. High Energy Phys. 02 (2015) 072.
[126] S. Antusch and O. Fischer, J. High Energy Phys. 05 (2015) 053.
[127] S. Banerjee, P. S. B. Dev, A. Ibarra, T. Mandal, and M. Mitra, Phys. Rev. D **92**, 075002 (2015).
[128] E. Arganda, M. J. Herrero, X. Marcano, and C. Weiland, Phys. Lett. B **752**, 46 (2016).
[129] A. Das, P. Konar, and S. Majhi, J. High Energy Phys. 06 (2016) 019.
[130] G. Aad *et al.* (ATLAS Collaboration), J. High Energy Phys. 07 (2015) 162.
[131] G. Bambhaniya, J. Chakrabortty, J. Gluza, M. Kordiaczyńska, and R. Szafron, J. High Energy Phys. 05 (2014) 033.
[132] G. Belanger, F. Boudjema, D. London, and H. Nadeau, Phys. Rev. D **53**, 6292 (1996).
[133] J. Gluza and M. Zrałek, Phys. Rev. D **52**, 6238 (1995).
[134] J. Gluza and M. Zrałek, Phys. Lett. B **362**, 148 (1995).
[135] T. Asaka and T. Tsuyuki, Phys. Rev. D **92**, 094012 (2015).
[136] B. W. Lee and R. E. Shrock, Phys. Rev. D **16**, 1444 (1977).
[137] K. A. Olive *et al.* (Particle Data Group), Chin. Phys. C **38**, 090001 (2014).
[138] A. M. Baldini *et al.*, arXiv:1301.7225.
[139] T. Aushev *et al.*, arXiv:1002.5012.
[140] L. Bartoszek *et al.* (Mu2e Collaboration), arXiv: 1501.05241.
[141] J.-P. Bu, Y. Liao, and J.-Y. Liu, Phys. Lett. B **665**, 39 (2008).
[142] P. Langacker and D. London, Phys. Rev. D **38**, 907 (1988).
[143] F. del Aguila, J. A. Aguilar-Saavedra, and M. Zrałek, Comput. Phys. Commun. **100**, 231 (1997).
[144] L. Wolfenstein, Phys. Lett. B **107**, 77 (1981).
[145] J. Gluza, T. Jelinski, and R. Szafron, arXiv:1604.01388.
[146] R. Allahverdi, B. Dutta, and R. N. Mohapatra, Phys. Lett. B **695**, 181 (2011).
[147] J. W. F. Valle and C. A. Vaquera-Araujo, Phys. Lett. B **755**, 363 (2016).
[148] T. Yanagida, Prog. Theor. Phys. **64**, 1103 (1980).
[149] R. N. Mohapatra and G. Senjanovic, Phys. Rev. D **23**, 165 (1981).
[150] M. Magg and C. Wetterich, Phys. Lett. B **94**, 61 (1980).
[151] R. Foot, H. Lew, X. G. He, and G. C. Joshi, Z. Phys. C **44**, 441 (1989).
[152] E. T. Franco, Phys. Rev. D **92**, 113010 (2015).
[153] M. B. Gavela, T. Hambye, D. Hernandez, and P. Hernandez, J. High Energy Phys. 09 (2009) 038.
[154] P. S. B. Dev and A. Pilaftsis, Phys. Rev. D **86**, 113001 (2012).
[155] P. S. Bhupal Dev and A. Pilaftsis, Phys. Rev. D **87**, 053007 (2013).
[156] R. L. Awasthi, M. K. Parida, and S. Patra, J. High Energy Phys. 08 (2013) 122.
[157] F. del Aguila, J. A. Aguilar-Saavedra, and R. Pittau, J. High Energy Phys. 10 (2007) 047.